REPRINTED FROM

JIST

JOURNAL OF IMAGING SCIENCE AND TECHNOLOGY

VOL. 60, NO. 5 | SEPTEMBER/OCTOBER 2016

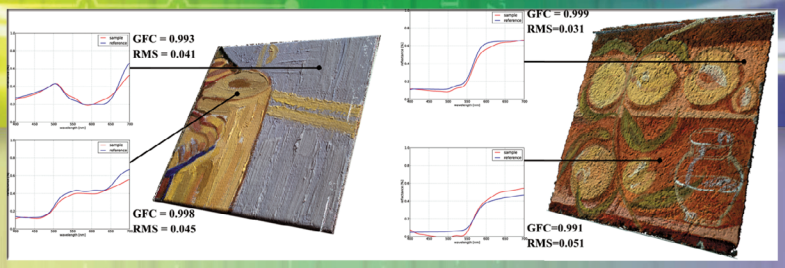

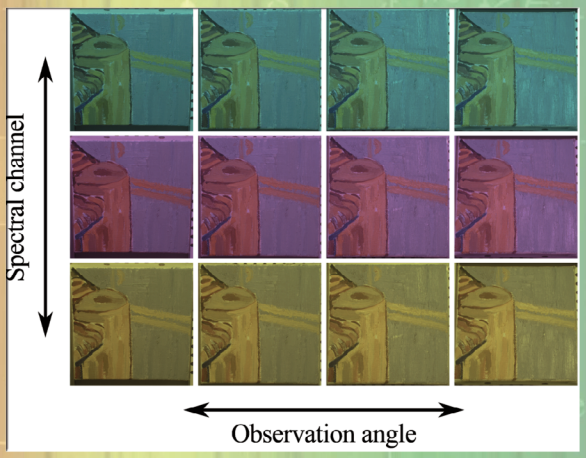

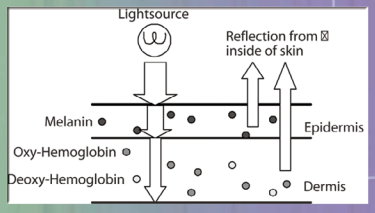

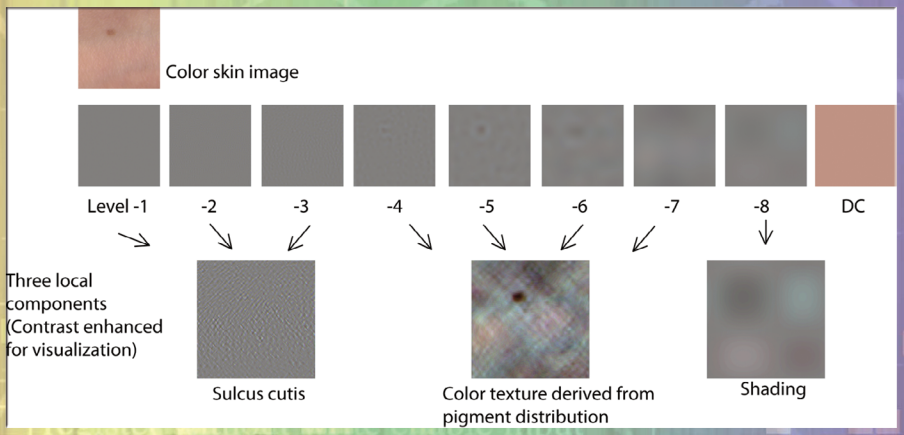

IS&T
imaging.org

Journal of Imaging Science and Technology® 60(5): 050406-1–050406-6, 2016.

Random Color Filter Arrays are Better than Regular Ones

Prakhar Amba
Laboratoire de Psychologie et NeuroCognition, CNRS UMR 5105, Univ. Grenoble Alpes, Grenoble, France

Jérôme Dias
Laboratoire de Psychologie et NeuroCognition, CNRS UMR 5105, Univ. Grenoble Alpes, Grenoble, France
ORME Signals & Images, Toulouse, France

David Alleysson
Laboratoire de Psychologie et NeuroCognition, CNRS UMR 5105, Univ. Grenoble Alpes, Grenoble, France
E-mail: David.Alleysson@upmf-grenoble.fr

Abstract. *Most of digital cameras today use a color filter array (CFA) and a single sensor to acquire color information of the scene. In this article, we ask which arrangement of colors in the mosaic of the CFA provides the best encoding of the scene. As a solution of the inverse problem of demosaicing, we consider a linear minimum mean squared error model. We used redundancy given by the neighborhood on the sampled image to ensure the stability of the solution. For some CFAs, LMMSE with neighborhood provides equivalent reconstruction results and less variability among the image content compared to edge-directed demosaicing on the Bayer. LMMSE allows comparing CFAs of regular pattern with random ones. We show that mosaics with random arrangement of colors and quasi equal proportion of RGB provide best reconstruction performance.* © *2016 Society for Imaging Science and Technology.*
[DOI: 10.2352/J.ImagingSci.Technol.2016.60.5.050406]

INTRODUCTION

A color image is composed with the intensity of three different channels covering three different domains of wavelength, usually in the Red, Green and Blue part of the visible spectrum. To acquire such an image with simplicity and low cost, a single sensor is used which is covered with a color filter array (CFA) to provide several color components to the acquired image, arranged in a mosaic. Thus only a single color is sampled at each pixel and reconstruction of missing colors (called demosaicing or demosaicking) is required.

The Bayer's CFA[1] is the most commonly used CFA and several methods have been proposed for improving the quality of the reconstruction. Edge-directed[2] methods which interpolate along contours and avoid interpolation across them are known to be the best method for the Bayer CFA. These methods are usually followed by a post-processing that improves the reconstructed image.[3–10] But the computation time needed for these methods makes them generally too costly for embedded systems. Moreover in practice, the CFA image produced by a sensor is less constraining than the simulated image on the Kodak database[11] (the most used one on demosaicing) which contains moiré due to higher frequency content compared to the number of pixels. This is even worse for recent cameras with small pixels size.[12] Because these methods are optimized for Bayer CFA they are not very useful for general CFAs such as those with random arrangement of color.

Some studies show new CFA patterns, but either they are designed empirically.[13–15] Many authors have proposed optimal CFAs arrangement based on the criteria of frequency representation and selection.[16–20] Indeed, the mosaic arrangement of the filters in the CFA could be interpreted as a spatial multiplexing of color components and has a simple expression in the Fourier domain.[21–23] The spatial Fourier representation of the CFA allows simple linear demosaicing by selecting the part of the spectrum that corresponds to luminance and color components. Some authors assume the RGB filter's spectral sensitivity can be modified and consider composed colors as a linear combination of RGB and propose an arrangement of these new colors that optimize the frequency representation and estimation. But there is no evidence that these new colors can be easily produced from physical composition of the RGB pigments. In addition, the simple mathematical expression of spatial multiplexing is due to periodicity or regularity in the mosaic. The locality of chrominance is lost for a random arrangement of color on the CFA. This prevents the application of frequency selection method on random CFAs.

Demosaicing is an inverse problem to retrieve the missing colors from the sampled ones. This problem has no general solution. To solve it, we must consider a model of the solution family (solutions appear as a functional for which a set of parameters are optimal for the problem) and provide the best estimated solution inside this family. It is almost straightforward to consider linear solutions.[24] We therefore restrict here the solutions to be linear application from $\mathbb{R}^n$ to $\mathbb{R}^m$, n will be the dimension of the mosaiced image plus neighborhood's space and m the dimension of the

Received Apr. 8, 2016; accepted for publication June 20, 2016; published online Aug. 18, 2016. Associate Editor: Yeong-Ho Ha.
1062-3701/2016/60(5)/050406/6/$25.00

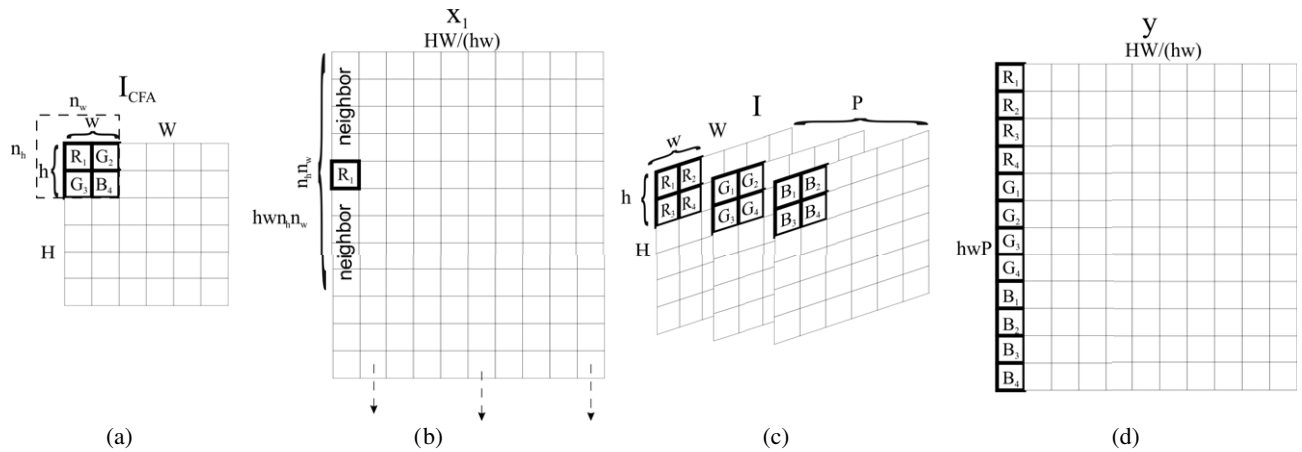

Figure 1. Detail of the unfolding of images into vectors (a) Mosaiced image I_{CFA} with a neighborhood shown (b) Unfolding of the mosaiced image into matrix $\boldsymbol{x}_1$ (c) Color image I (d) Unfolding of the color image into matrix $\boldsymbol{y}$.

reconstructed color image's space (See next section for detail on the image formation model).

A general linear approach for demosaicing consists of minimizing the squared error of reconstruction and derives a linear least square approximation of the solution.[25,26] This method is general and applies equally well to any CFA. Because most of the CFAs are a replication of a basis pattern, a shift invariant solution can be found, which simplifies calculation by considering only the basis pattern (called super-pixel) replicated on the surface of the CFA, a 2×2 array for Bayer's pattern.[26,27] Despite the generality of the method which allows optimizations,[28–30] the solution obtained with such a procedure is unstable because the number of unknowns is larger than the number of inputs. An elegant way for improving the number of inputs is to consider a closed neighborhood around the position to be interpolated. Intuitively, this reinforces the statistical learning of the solution with existing data and provides good reconstruction results.[31–36] This framework allows the use of a random pattern inside the super-pixel[37] even if the spatial frequency spectrum of luminance and chrominance for these CFAs is aliased.

Based on the LMMSE demosaicing we can directly compare the performance of any CFA pattern to reconstruct the desired image from the acquired image over a similar reconstruction method. In the next section, we describe the formalism for demosaicing with linear minimum mean square error, learning over a database with generalized neighborhood. We then compare the performance of several CFAs. We also show the comparative performance with some of the state of the art methods applying on Bayer CFA.

LINEAR MODEL OF IMAGE FORMATION

Writing a matrix model of image formation requires unfolding the matrix representing images into vectors, then finding a matrix–vector multiplication that relates the expected image from the acquired one.[26] In the case of demosaicing we suppose that the mosaiced image results from a color image multiplied by a projection matrix.[32] But there are many ways of unfolding images that results in different models.

Classically an image is unfolded into a column vector. For the demosaicing problem it is expressed as follows: consider a color image I having H rows, W columns and P color channels and the mosaiced image I_{CFA} having H rows and W columns. We can construct the column vector $\mathbf{y}$ of size PHW $\times$ 1 corresponding to the color image and $\mathbf{x}$ of size HW $\times$ 1 corresponding to the mosaiced image (Figure 1).[26] In this case the model of image formation can be expressed as:

$$\mathbf{x} = \boldsymbol{M}\mathbf{y} \tag{1}$$

where $\boldsymbol{M}$ is a HW $\times$ PHW matrix that transforms the vector $\mathbf{y}$ corresponding to a color image into a vector $\mathbf{x}$ corresponding to the mosaiced image.

The demosaicing matrix $\boldsymbol{D}$, we wish to estimate is the reverse operator that gives the estimate $\hat{\mathbf{y}}$ from $\mathbf{x}$. It can be calculated from several couples $(\mathbf{x}, \mathbf{y})_i$ constructed from a database with the Wiener filtering approach that corresponds to the least square error estimator.

$$\boldsymbol{D} \quad \text{such that } \hat{\mathbf{y}} = \boldsymbol{D}\mathbf{x}, \quad \boldsymbol{D} = E^{i=1\ldots k}\{\mathbf{y}\mathbf{x}^t(\mathbf{x}\mathbf{x}^t)^{-1}\}, \tag{2}$$

With $E^{i=1\ldots k}\{\}$ is the expectation over the k images of the database. In this model $\boldsymbol{D}$ is of size PHW $\times$ HW. This model implies huge matrices as a model because the dimension of $\boldsymbol{M}$ or $\boldsymbol{D}$ is of size of the number of pixels in the images.

A better model is given by considering the block shift invariant property of the mosaic. Since the mosaic is composed by a super-pixel of size $h \times w$ replicated on the whole CFA of size $H \times W$, we can unfold the image for hw instead of HW. In this case the model formulation (Eq. (1)) remains the same but $\boldsymbol{y}$ is now a $Phw \times \mathrm{HW}/(hw)$ matrix containing the set of vectors built from one super-pixel in the color image. And $\boldsymbol{x}$ is a $hw \times \mathrm{HW}/(hw)$ matrix corresponding to the set of vectors built from one super-pixel of the mosaiced image. Thus $\boldsymbol{M}$ is a $hw \times Phw$ matrix (i.e. 4×12 for the 2×2 super-pixel of the Bayer CFA) and $\boldsymbol{D}$ is a $Phw \times hw$ matrix[31,32] which greatly reduces the

computational complexity required to calculate $\boldsymbol{D}$ and apply the reconstruction to the acquired data. But, with this model, the number of values to be retrieved is P times larger than the acquired values making the estimate quite unstable.

To reinforce the stability of the solution, a neighborhood of $\mathbf{x}$ could be used. Let $\mathbf{x}_1$ be a vector built from $\mathbf{x}$ and its close neighborhood of size $n_h \times n_w$, $\mathbf{x}_1 = N_{n_h,n_w}(\mathbf{x})$. $N_{n_h,n_w}(.)$ is a function that increase the number of rows of a vector by the $n_h \times n_w$ neighbors of each element of the vector. In this case, $\mathbf{x}_1$ is of size $hwn_hn_w \times \mathrm{HW}/(hw)$ and the number of rows of $\mathbf{x}_1$ could be easily larger than Phw.

In this later unfolding, the computation of the demosaicing matrix from couples $(\mathbf{x}_1, \mathbf{y})_i$ constructed from the database is given by the following equation:

$$\boldsymbol{D} \quad \text{such that } \hat{\mathbf{y}} = \boldsymbol{D}\mathbf{x}_1, \qquad \boldsymbol{D} = E^{i=1\ldots k}\{\mathbf{y}\mathbf{x}_1^t(\mathbf{x}_1\mathbf{x}_1^t)^{-1}\}. \quad (3)$$

Similar to the Eq. (1), it is possible to design a matrix $\boldsymbol{M}_1$ that transform a neighborhood in the color image (vector $\mathbf{y}_1$) into a neighborhood of the mosaiced image $\mathbf{x}_1$, i.e. $\mathbf{x}_1 = \boldsymbol{M}_1\mathbf{y}_1$. It is also possible to design a matrix $\boldsymbol{S}_1$ that transforms the vector $\mathbf{y}_1$ into the vector $\mathbf{y}$, i.e. $\mathbf{y} = \boldsymbol{S}_1\mathbf{y}_1$, such that it suppresses the neighborhood and selects the central pattern. With these two matrixes, $\boldsymbol{D}$ can be expressed as:

$$\boldsymbol{D} = \boldsymbol{S}_1 R\boldsymbol{M}_1^t(\boldsymbol{M}_1 R\boldsymbol{M}_1^t)^{-1}, \qquad \text{with } R = E^i\{\mathbf{y}_1\mathbf{y}_1^t\}. \quad (4)$$

Equation (4) implies that we need to calculate the correlation R only once from the color images with their neighborhoods in the database. Then, for a particular CFA into consideration, we can construct $\boldsymbol{M}_1$ and $\boldsymbol{S}_1$ and compute the optimal demosaicing filter in the least square sense. Thus, with the same R we can compare the performance of any CFA.

In Ref. [33] a similar notation to Eq. (4) is provided, but the neighborhood size is restricted to an integer number of the size of the super-pixel which becomes intractable when super-pixel size increase and is less flexible. Here, we proposed a generalization for any CFA with any super-pixel size and any arrangement of colors inside the super-pixel. The construction of $\boldsymbol{M}_1$ and $\boldsymbol{S}_1$ for a particular arrangement and a particular neighborhood is not trivial and cannot be described more here.

SIMULATION

With the framework given in the previous section, we can easily compare the performance of several CFAs with any super-pixel size and any arrangement of colors inside the super-pixel as well as any size of the neighborhood used for controlling redundancy. The framework works as follows: for any color image taken from the database, we compute $\mathbf{y}_1$, composed by the set of vectors constructed for every pixel inside the super-pixels and theirs neighbors. From all $\mathbf{y}_1$ taken from all images in the database, we compute R according to Eq. (4). Then we design $\boldsymbol{S}_1$ and $\boldsymbol{M}_1$ for the CFA and the neighborhood size. We compute $\boldsymbol{D}$ with Eq. (4).

The performance of the demosaicing is then computed as follows: for each image in the database, we compute the mosaiced image by subsampling the color image according to the CFA. Then we compute the vector $\mathbf{x}_1$ using the neighborhood. We apply $\boldsymbol{D}$ on $\mathbf{x}_1$ as in Eq. (3) to reconstruct the estimate $\hat{\mathbf{y}}$ and compare it to $\mathbf{y}$ by calculating PSNR (A border equivalent to neighborhood size was removed in the calculation).

We compute a PSNR from the whole mean square difference between the original and reconstructed image for all pixels and three PSNRs, one per color channel. We use the average of whole PSNR over all the images in the database, μ as an estimator of the overall quality of the reconstruction. The variance of the whole PSNR along image number, σ gives an estimate of the adequacy of the method to encode any particular image. To test the method to equally encode any colors, we used the average of the PSNR per channel, μ_R, μ_G and μ_B as well as the average of the variance of PSNR per channel, σ_{RGB}. Finally, the SSIM[38] (computed the three channels together) is also provided to estimate the quality of the image in term of visual factors.

We perform the analysis on two databases (Kodak,[11] McM[39]) for comparing the performances. The Kodak database is known to have much higher frequency compared to the number of pixels and with low colorfulness which favor the edge-directed and post-processing methods. The McM database has been proposed as having more realistic images in term of high frequency and colorfulness. We generally used all the images from the database for learning the demosaicing operator. We also implement a leave-one-out simulation where the image to reconstruct is not in the set of images used to learn which are presented in supplementary material.[42]

Systematic evaluation for 2×2, 3×3 *super-pixel size of the CFA*

As a first example of performance comparison, we consider all the different combination of three colors R, G, B on a 2×2 super-pixel. The number of different possible arrangements is $3^4 = 81$. However, notice that a lot of them are symmetrical than others. We also consider all the different combinations of the 3×3 super-pixel, there are $3^9 = 19,683$ different ones.

Table I and Figure 3 (top row) shows the best 2×2 arrangements calculated over the Kodak databases. In term of average PSNR, μ, the best arrangement is not the Bayer RG; GB but slightly modified one where the arrangement is RG; BG (2×2 #1). If we look at the average variance between PSNR calculated on individual color channels in the reconstructed images over the database, σ_{RGB}, the best is RB; GB (2×2 #2) arrangement. Also, if we look at the average variance of the overall PSNR, σ, along all the images in the database, the BR; GG (2×2 #3) is the best. This shows the following criterion that either twice of green or blue is preferred but the color represented twice is never on the diagonal.

Table I and Fig. 3 (top row) also shows the result for evaluating all the different 3×3 CFAs. Again depending on the criterion (μ, σ_{RGB}, σ) three different optimal ones are

Table I. Comparison of CFA for Kodak database, $nh = nw = 10$.

CFA	Kodak						
	μ	μ_R	μ_G	μ_B	σ_{RGB}	σ	SSIM
Bayer	38.90	38.57	41.53	37.59	4.64	6.57	0.9911
2 × 2 #1	**39.51**	39.41	40.36	38.99	1.01	7.21	0.9923
2 × 2 #2	39.10	38.71	39.39	39.32	**0.53**	7.64	0.9917
2 × 2 #3	39.12	38.27	40.27	39.22	1.78	**5.01**	0.9916
3 × 3 #1	37.16	37.40	37.13	37.02	**0.22**	6.34	0.9881
3 × 3 #2	**38.96**	38.70	39.48	38.78	0.39	6.81	0.9913
3 × 3 #3	36.36	37.40	35.81	36.13	1.11	**5.41**	0.9859
4 × 4 #1	40.26	40.51	40.32	40.05	0.40	6.44	0.9933
4 × 4 #2	**40.40**	41.00	39.82	40.56	0.76	6.39	**0.9936**
Yaman.	38.73	37.82	40.95	38.19	3.46	6.81	0.9910
Lukac	39.35	38.70	41.47	38.57	3.13	6.31	0.9918
Holladay	38.57	39.23	39.62	37.30	1.87	6.05	0.9908
Cnrs	39.78	40.01	40.02	39.39	0.40	6.42	0.9927

shown. Among these three no one is regular and all three show an almost equal number of RGB.

Figure 2 shows the histogram of the average PSNR, μ, for all of 3 × 3 CFAs. The three first peaks correspond to CFA with only one or two colors. As shown in Fig. 2(b), among the best hundred 3 × 3 CFAs, some are symmetrical but none are perfectly regular.

Comparison of CFAs under LMMSE

We select several CFAs (Fig. 3) proposed in the literature that we have tested with LMMSE demosaicing. We also compute the best arrangement of the 4 × 4 (they are $3\hat{}16 > 43$ Millions) by pruning those with high bias between colors based on the previous results for 3 × 3 and 2 × 2. We also add the best 2 × 2 and the original Bayer in the comparison. Figure 4 shows the performance of CFAs along the neighborhood size, which clearly favor the best 4 × 4 #2 for a neighborhood of size larger than 3. This CFA is also performing well with variance estimators showing its ability to equally encode colors and perform well for any image in the database.

Table I shows the number of the evaluation parameter estimated based on a neighborhood of 10 × 10 for the CFAs. In the table we highlight the number that is the best within that category. For example, the best 2 × 2 for average PSNR, μ is given for the 2 × 2 #1. We show the result for the 4 × 4 #1 because even if it is not the best for average PSNR, it has very good visual performance on the fence of the lighthouse image as shown in the supplementary material.

Comparison with other methods on Bayer

We compare the best 4 × 4 using a neighborhood of 10 with the state of the art method applying on the Bayer CFA using both the Kodak and McM database. The following Tables II and III show the evaluation parameters as well as the computation time on Matlab. The code for the algorithms is found on web site.[40]

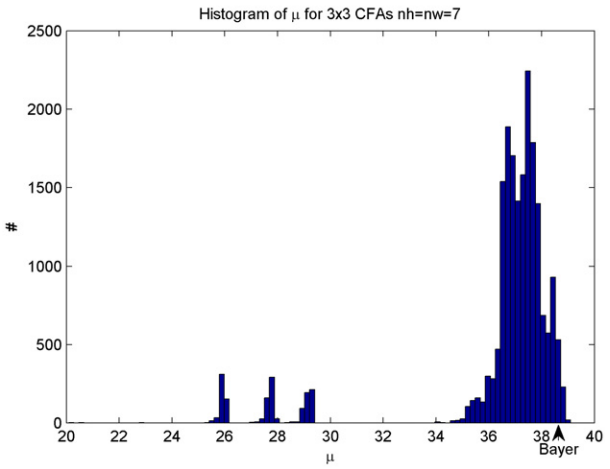

(a)

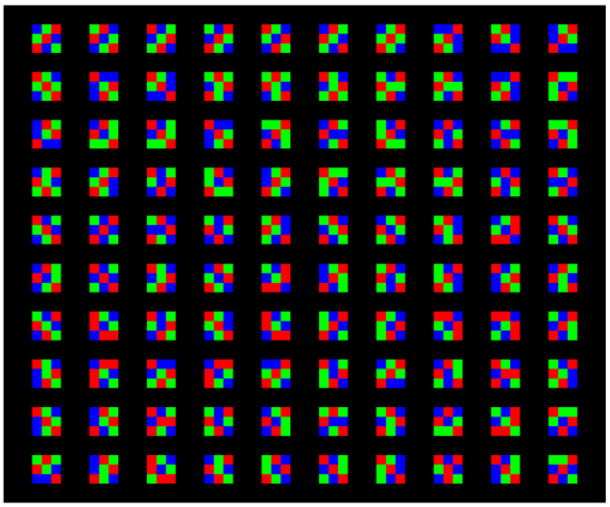

(b)

Figure 2. (a) Histogram of the PSNR for all 3 × 3 CFAs. A large number of them show more than 38dB of average PSNR. (b) The top hundred 3 × 3 CFA's for average PSNR learned over the Kodak database (The PSNR ranges between 38.96 and 38.70 for the top hundred for neighborhood of 10 for Kodak database). See supplementary material for the result on McM.

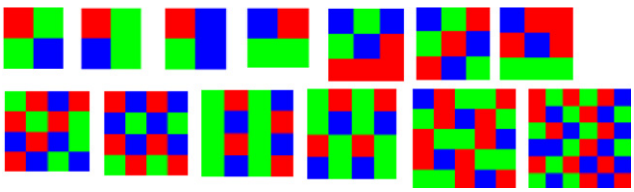

Figure 3. Different CFA pattern used for comparison. From left to right top row, Bayer, 2 × 2 #1, 2 × 2 #2, 2 × 2 #3, 3 × 3 #1, 3 × 3 #2, 3 × 3 #3, bottom row, 4 × 4 #1, 4 × 4 #2, Yamanaka,[14] Lukac,[13] Holladay halftone,[30] CNRS.[15]

For the Kodak database, the best 4 × 4 has almost the same performance as the best edge-directed method with a far less variance between colors. It has also a better variance among images on the database as well as SSIM[38] and computation time per image. For the MCM database, the best 4 × 4 under LMMSE perform better than any other in the

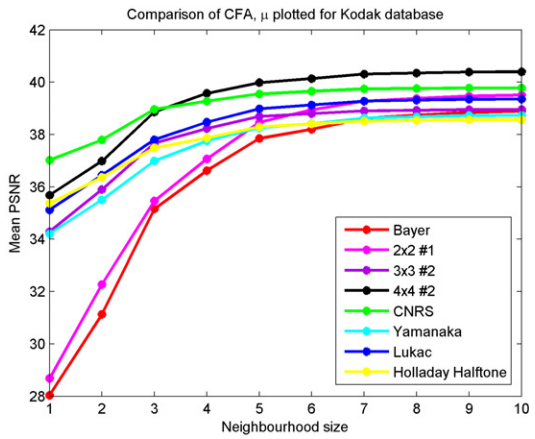

(a)

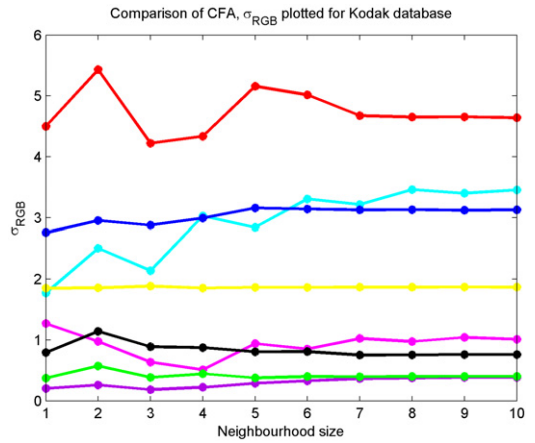

(b)

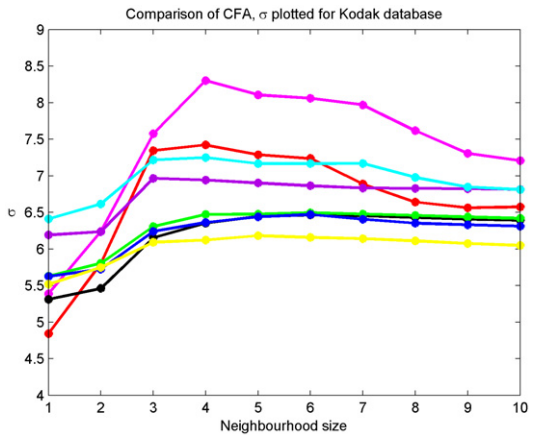

(c)

Figure 4. Evaluation of CFAs with LMMSE with increasing neighborhood (a) Average PSNR, μ. (b) Variance of PSNR per channel, σ_{RGB}. (c) Variance of PSNR with image number, σ.

test for almost all these performance parameters (Table III). The supplementary material shows some examples of reconstruction based on particular area on images.

For sure the extent of the size of the super-pixel provides a better encoding of the scene as shown by the objective criteria such the PSNR. But in our simulations, we also see that the random arrangement of colors in the CFA also reduces the visibility of the noise generated by the mosaicing/demosaicing process because noise becomes less structured.

Table II. Comparison between the best 4 × 4 with LMMSE on Kodak database and other methods.

Method	Kodak							
	μ	μ_R	μ_G	μ_B	σ_{RGB}	σ	SSIM	Time (s)
4 × 4 #1	40.26	40.51	40.32	40.05	**0.40**	6.44	0.9933	0.64
4 × 4 #2	40.40	**41.0**	39.82	**40.6**	0.76	6.39	**0.9936**	0.65
LPA-ICI	**40.52**	39.63	**43.0**	39.91	4.45	7.08	0.9874	1.15
LIAN	39.53	38.59	42.13	38.86	4.63	7.39	0.9855	0.31
DA	37.82	37.38	40.66	36.54	5.27	5.82	0.9829	0.09
HD	37.72	36.94	39.59	37.26	2.82	8.64	0.9799	28.11
SA	39.01	37.92	41.56	38.53	4.57	6.37	0.9850	1.30
DFPD	39.17	38.32	41.23	38.70	3.25	7.83	0.9837	1.55
DLMMSE	40.05	39.12	42.58	39.53	4.79	6.92	0.9866	28.84
AP	39.25	38.29	41.73	38.70	4.40	**6.07**	0.9849	1.61
LI	35.66	35.16	38.83	34.25	6.05	10.24	0.9729	**0.02**
HA	36.87	36.75	38.05	36.08	1.20	10.40	0.9769	0.08
Bilinear	30.19	29.25	33.07	29.26	4.94	10.94	0.9160	0.04

Table III. Comparison between the best 4 × 4 with LMMSE on McM database and other methods.

Method	McM							
	μ	μ_R	μ_G	μ_B	σ_{RGB}	σ	SSIM	Time (s)
4 × 4 #1	35.44	36.96	35.89	34.14	2.83	9.32	0.9832	0.39
4 × 4 #2	**35.96**	**37.3**	35.55	**35.4**	**1.84**	9.33	**0.9851**	0.40
LPA-ICI	34.70	34.32	37.88	33.29	6.62	13.20	0.9655	0.64
LIAN	34.91	34.55	37.95	33.52	6.13	10.40	0.9673	0.17
DA	32.22	31.82	34.69	31.07	4.16	13.33	0.9528	0.06
HD	33.46	32.94	36.96	32.15	7.94	11.20	0.9576	18.50
SA	32.69	32.56	34.42	31.70	2.71	17.88	0.9529	0.87
DFPD	34.22	33.74	37.17	32.96	5.64	10.77	0.9624	0.99
DLMMSE	34.43	33.97	**37.9**	33.02	7.93	11.21	0.9647	18.27
AP	33.14	32.79	35.13	32.17	3.01	12.47	0.9567	1.03
LI	34.39	33.94	37.52	32.97	6.03	**8.75**	0.9645	**0.02**
HA	34.79	34.58	**37.9**	33.27	6.87	9.96	0.9654	0.05
Bilinear	32.29	31.65	35.38	31.20	6.59	11.58	0.9487	0.03

LPA-ICI,[3] LIAN,[41] DA,[21] HD,[4] SA,[5] DFPD,[6] DLMMSE,[7] AP,[8] LI,[9] HA,[2] are tested with a border of 15, 4 × 4 #1 and 4 × 4 #2 reported with a border of 10.

CONCLUSION

In this article we provide a flexible, fast and accurate linear minimum mean squared error demosaicing using the redundancy given by the neighborhood of the sampled image. The method is quite fast and allows us to systematically compare the performance of 2 × 2 and 3 × 3 CFA's super-pixels and most of the 4 × 4 CFAs.

Compared to frequency selection approaches used today for optimizing CFAs, our method does not guess the frequency spectrum of the sampled image by the CFA.

Rather, it uses a learning procedure that computes optimal reconstruction filters. Even when the aliasing between luminance and chrominance is strong (as arising for random pattern), the method finds good linear reconstruction filters. We found that the best CFAs are the ones with non-regular arrangement of colors (some are symmetric along the $\pm 45°$ line) and almost equal number of RGB.

The best known methods for demosaicing are thought to be those with edge-directed interpolation and post-processing. We show that the 4×4 best CFAs give reconstruction results equivalent to the best nonlinear algorithms applied on Bayer. It even provides less variability among colors and particular image in the database. Moreover, it gives better SSIM evaluation for a less computation time. This result provides linear demosaicing for being favorably used in the embedded camera devices.

Statistics of natural images are probably random because a contour or a particular object's color could potentially appear anywhere on the images. That is probably why random CFA perform better than regular one for encoding the spatial and chromatic structure of natural images.

ACKNOWLEDGMENT

This work is financed by the FUI Extrem OWL no. F1411026U to P. Amba and D. Alleysson.

REFERENCES

[1] B. E. Bayer, US Patent 3,971,065. Washington, DC: US Patent and Trademark Office (1976).
[2] J. F. Hamilton Jr and J. E. Adams, "Adaptive color plane interpolation in single color electronic camera", US Patent 5 629 734 (1997).
[3] D. Paliy, V. Katkovnik, R. Bilcu, S. Alenius, and K. Egiazarian, "Spatially adaptive color filter array interpolation for noiseless and noisy data," Int. J. Imaging Syst. Technol. **17**, 105–122 (2007).
[4] K. Hirakawa and T. W. Parks, "Adaptive homogeneity-directed demosaicing algorithm," IEEE Trans. Image Process. **14**, 360–369 (2005).
[5] X. Li, "Demosaicing by successive approximation," IEEE Trans. Image Process **14** (2005).
[6] D. Menon, S. Andriani, and G. Calvagno, "Demosaicing with directional filtering and a posteriory decision," IEEE Trans. Image Process. **16**, 132–141 (2007).
[7] L. Zhang and X. Wu, "Color demosaicking via directional linear minimum mean square-error estimation," IEEE Trans. Image Process. **14**, 2167–2178 (2005).
[8] B. K. Gunturk, Y. Altunbasak, and R. M. Mersereau, "Color plane interpolation using alternating projections," IEEE Trans. Image Process. **11**, 997–1013 (2002).
[9] H. S. Malvar, L.-W. He, and R. Cutler, "High-quality linear interpolation for demosaicing of Bayer-patterned color images," *Proc. IEEE Int'l. Conf. Acoustics, Speech, and Signal Processing (ICASSP '04)* (IEEE, Piscataway, NJ, 2004), Vol. 3, pp. 485–488.
[10] A. Hore and D. Ziou, "An edge-sensing generic demosaicing algorithm with application to image resampling," IEEE Trans. Image Process. **20**, 3136–3150 (2011).
[11] Kodak Database http://r0k.us/graphics/kodak/.
[12] F. Yasuma, T. Mitsunaga, D. Iso, and S. K. Nayar, "Generalized assorted pixel camera: postcapture control of resolution, dynamic range, and spectrum," IEEE Trans. Image Process. **19**, 2241–2253 (2010).
[13] R. Lukac and K. Plataniotis, "Color filter arrays: design and performance analysis," IEEE Trans. Consum. Electron. **51**, 1260–1267 (2005).
[14] S. Yamanaka, "Solid state camera", US Patent 4,054,906, (1977).
[15] D. Alleysson, B. C. de Lavarène, and J. Herault, US Patent 8,564,699. Washington, DC: US Patent and Trademark Office (2013).
[16] L. Condat, "A new color filter array with optimal sensing properties," *16th IEEE Int'l. Conf. on Image Processing (ICIP), 2009* (IEEE, Piscataway, NJ, 2009), pp. 457–460.
[17] K. Hirakawa and P. J. Wolfe, "Spatio-spectral color filter array design for optimal image recovery," IEEE Trans. Image Process. **17**, 1876–1890 (2008).
[18] C. Bai, J. Li, Z. Lin, and J. Yu, "Automatic design of color filter arrays in the frequency domain," IEEE Trans. Image Process. **25**, 1793–1807 (2016).
[19] P. Hao, Y. Li, Z. Lin, and E. Dubois, "A geometric method for optimal design of color filter arrays," IEEE Trans. Image Process. **20**, 709–722 (2011).
[20] J. Couillaud, A. Horé, and D. Ziou, "Nature-inspired color-filter array for enhancing the quality of images," J. Opt. Soc. Am. A **29**, 1580–1587 (2012).
[21] D. Alleysson, S. Süsstrunk, and J. Hérault, "Color demosaicing by estimating luminance and opponent chromatic signals in the Fourier domain," *Proc. IS&T/SID Tenth Color Imaging Conf.* (IS&T, Springfield, VA, 2002), Vol. 2002, pp. 331–336.
[22] D. Alleysson, S. Süsstrunk, and J. Hérault, "Linear demosaicing inspired by the human visual system," IEEE Trans. Image Process. **14**, 439–449 (2005).
[23] E. Dubois, "Frequency-domain methods for demosaicking of Bayer-sampled color images," IEEE Signal Process. Lett. **12**, 847 (2005).
[24] A. Ribes and F. Schmitt, "Linear inverse problems in imaging," IEEE Signal Process. Mag. **25**, 84–99 (2008).
[25] H. J. Trussell, "A MMSE estimate for demosaicking," *Proc. 2001 Int'l. Conf. on Image Processing, 2001* (IEEE, Piscataway, NJ, 2001), Vol. 3, pp. 358–361.
[26] H. J. Trussell and R. E. Hartwig, "Mathematics for demosaicking," IEEE Trans. Image Process. **11**, 485–492 (2002).
[27] D. Taubman, "Generalized wiener reconstruction of images from colour sensor data using a scale invariant prior," *Proc. 2000 Int'l. Conf. Image Processing, 2000* (IEEE, Piscataway, NJ, 2000), Vol. 3, pp. 801–804.
[28] M. Parmar and S. J. Reeves, "A perceptually based design methodology for color filter arrays [image reconstruction]," *Proc. IEEE Int'l. Conf. on Acoustics, Speech, and Signal Processing, 2004 (ICASSP'04)* (IEEE, Piscataway, NJ, 2004), Vol. 3, pp. iii–473.
[29] M. Parmar and S. J. Reeves, "Selection of optimal spectral sensitivity functions for color filter arrays," *IEEE Int'l. Conf. Image Processing, 2006* (IEEE, Piscataway, NJ, 2006), pp. 1005–1008.
[30] M. Parmar and S. J. Reeves, "Selection of optimal spectral sensitivity functions for color filter arrays," IEEE Trans. Image Process. **19**, 3190–3203 (2010).
[31] B. C. de Lavarène, D. Alleysson, and J. Hérault, "Practical implementation of LMMSE demosaicing using luminance and chrominance spaces," Comput. Vis. Image Underst. **107**, 3–13 (2007).
[32] D. Alleysson, B. C. de Lavarène, S. Susstrunk, and J. Hérault, "Linear minimum mean square error demosaicking," *Single-Sensor Imaging: Methods and Applications for Digital Cameras* (CRC Press, Inc. Boca Raton, FL, USA, 2008), pp. 213–237, ISBN 142005452X 9781420054521.
[33] Y. M. Lu and M. Vetterli, "Optimal color filter array design: quantitative conditions and an efficient search procedure," Proc. SPIE **7250**, 725009 (2009).
[34] Y. M. Lu, C. Fredembach, M. Vetterli, and S. Süsstrunk, "Designing color filter arrays for the joint capture of visible and near-infrared images," *16th IEEE Int'l. Conf. on Image Processing (ICIP), 2009* (IEEE, Piscataway, NJ, 2009), pp. 3797–3800.
[35] Z. Sadeghipoor, Y. M. Lu, and S. Süsstrunk, "Correlation-based joint acquisition and demosaicing of visible and near-infrared images," *18th IEEE Int'l. Conf. Image Processing (ICIP), 2011* (IEEE, Piscataway, NJ, 2011), pp. 3165–3168.
[36] Z. Sadeghipoor, Y. M. Lu, and S. Süsstrunk, "Optimum spectral sensitivity functions for single sensor color imaging," Proc. SPIE **8299**, 829904 (2012).
[37] D. Alleysson and B. C. de Lavarène, "Frequency selection demosaicking: a review and a look ahead," Proc. SPIE **6822**, 68221M (2008).
[38] Z. Wang, A. C. Bovik, H. R. Sheikh, and E. P. Simoncelli, "Image qualifty assessment: from error visibility to structural similarity," IEEE Trans. Image Process. **13**, 600–612 (2004).
[39] L. Zhang, X. Wu, A. Buades, and X. Li, "Color demosaicking by local directional interpolation and nonlocal adaptive thresholding," J. Electron. Imaging **20**, 023016 (2011).
[40] http://web.engr.illinois.edu/~khashab2/files/2013_2014_demosaicing/demosaicing.html.
[41] N.-X. Lian, L. Chang, Y.-P. Tan, and V. Zagorodnov, "Adaptive filtering for color filter array demosaicking," IEEE Trans. Image Process. **16** (2007).
[42] Supplementary material is available at http://david.alleysson.free.fr/CIC24/supplementarymaterial.pdf .

For information on reprints or reproduction contact
Donna Smith
Production Editor
The Journal of Imaging Science and Technology
Society for Imaging Science and Technology
7003 Kilworth Lane
Springfield, Virginia 22151 USA
703/642-9090 extension 107
703/642-9094 (fax)
dsmith@imaging.org
www.imaging.org